

# Semiconductor optical amplifier pattern effect suppression for return-to-zero data using an optical delay interferometer

**Kyriakos E. Zoiros**

Democritus University of Thrace  
School of Engineering  
Department of Electrical and Computer Engineering  
Lightwave Communications Research Group  
12 Vas. Sofias Str.  
67 100, Xanthi, Greece  
E-mail: kzoiros@ee.duth.gr

**Carlos L. Janer**

University of Limerick  
Department of Electronic and Computer  
Engineering  
Optical Communications Research Group  
Limerick, Ireland  
and  
Universidad de Sevilla  
Escuela Superior de Ingenieros  
Departamento de Ingeniería Electrónica  
Seville, Spain

**Michael J. Connelly**

University of Limerick  
Department of Electronic and Computer  
Engineering  
Optical Communications Research Group  
Limerick, Ireland

**Abstract.** An optical delay interferometer (ODI) is employed to suppress the pattern effect manifested on a 10 Gb/s return-to-zero (RZ) data stream when amplified by a semiconductor optical amplifier (SOA) operated in deep gain saturation. The experimental results verify the competence of the scheme to confront the problem for this signal format by achieving a far better performance than that with the SOA alone. © 2010 Society of Photo-Optical Instrumentation Engineers. [DOI: 10.1117/1.3481137]

Subject terms: semiconductor optical amplifier; pattern effect; return-to-zero data; optical delay interferometer.

Paper 100454R received Jun. 4, 2010; revised manuscript received Jul. 5, 2010; accepted for publication Jul. 7, 2010; published online Aug. 17, 2010.

## 1 Introduction

The technology of semiconductor optical amplifiers (SOAs) has evolved to the point that they have become indispensable elements in optical communications. However, the use of SOAs in their classical roles as power boosters,<sup>1</sup> in-line amplifiers,<sup>2-4</sup> and receiver preamplifiers<sup>5</sup> is limited by the pattern effect that occurs due to the strong saturation and incomplete recovery of their gain in between excitation pulses.<sup>6</sup> One method to alleviate this impairment is to convert the phase change that accompanies the amplified optical signal<sup>6</sup> to an amplitude modulation of the opposite magnitude to the SOA signal amplitude distortion, which compensates for the irregular gain variation. This can be achieved by means of interferometric structures; several versions have been proposed,<sup>7-9</sup> but they have been restricted to non-return-to-zero (NRZ) coding. In some practical applications, the return-to-zero (RZ) format is preferable in terms of receiver sensitivity and transmission performance.<sup>10</sup> In this case, the nature of the pattern effect phenomenon is different because it incurs fluctuations between the peak amplitudes of the data pulses<sup>11</sup> instead of overshoots at their leading edges.<sup>7-9</sup> Its impact on the

pulses is also more severe, because by definition their duration is shorter than the bit period, which in turn imposes a greater strain on the SOA gain dynamics. In this paper we tackled this demanding situation using an optical delay interferometer (ODI) and significantly reduced the pattern-dependent distortion on a 10-Gb/s RZ data pulse stream amplified by an SOA. Compared to the other schemes that we recently proposed for the same purpose,<sup>12,13</sup> the ODI has a similar comb-like transfer function<sup>14</sup> that is exploited to suppress the spectral components of the amplified signal broadened due to gain saturation.<sup>15</sup> However, the operation mechanism of our new scheme relies on the crosswise interference of the amplified signal with its delayed replica,<sup>11</sup> whereas that in Refs. 12 and 13 was based on polarization discrimination. Therefore, the ODI is less sensitive to changes in the polarization state of the input signal as opposed to that of Ref. 12. Also, it is compatible with planar waveguide technology<sup>14</sup> and can be integrated with the SOA on a single chip,<sup>16</sup> so it is a more compact option than that of Ref. 13. For these reasons, our new scheme can provide a practical solution to the pattern-effect problem and allow the amplification of RZ data by an SOA without performance degradation.

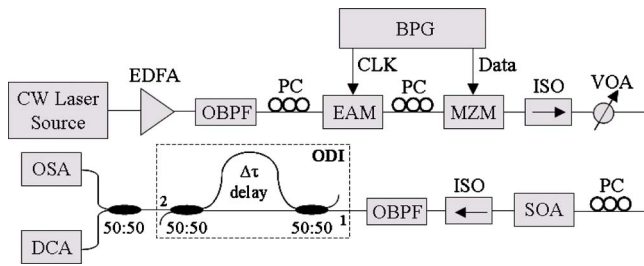


Fig. 1 Experimental setup.

## 2 Experiment

Figure 1 depicts the experimental setup for testing the potential of the proposed scheme to suppress the pattern effect induced on RZ pulses when they are directly amplified by an SOA. The RZ pulses were generated using an electroabsorption modulator (EAM) and a LiNbO<sub>3</sub> Mach-Zehnder modulator (MZM) in cascade, which were driven by the internally synchronized clock (CLK) and the data output of a bit pattern generator (BPG), respectively. The EAM first modulated a continuous wave (CW) signal generated by a tunable laser source at 1550 nm and boosted by an erbium-doped fiber amplifier (EDFA) to 17 dBm. This process produced a train of continuous optical pulses that were subsequently carved by the MZM to form a 10 Gb/s RZ 2<sup>7</sup>-1 pseudorandom binary sequence (PRBS) with a duty cycle of 31%. This encoded signal then passed through a variable optical attenuator (VOA) to control the power it sent to the SOA. The SOA was a 1-mm-long, bulk InGaAsP/InP device (Kamelian, model OPA-20-N-C-FA) with a fiber-to-fiber small-signal gain of 23 dB, a 3-dB saturation input power of -7 dBm, a gain polarization dependence of 0.5 dB, and a gain recovery time of approximately 75 ps at 1550 nm when biased at 270 mA and thermally stabilized at 20 °C. The amplified RZ data stream was launched into an ODI constructed by connecting two 3-dB, polarization-maintaining, fused couplers with a length difference between the upper and lower arms that resulted in a relative time delay  $\Delta\tau$ . The insertion loss (IL) of the ODI was measured to be 7 dB, which was lower than the ~8 dB and 8.5 dB measurements for the schemes proposed in Refs. 12 and 13, respectively. This difference is attributed to the fact that the structure and operation of the ODI are comparatively simpler, so the total contribution of the passive components involved in its construction to the IL parameter is smaller. Under the conditions of the conducted experiment, the SOA provided an amplification that made this signal attenuation practically tolerable. In the more general case, and regardless of the SOA functional characteristics, the IL introduced by the ODI can be further reduced if the latter is monolithically integrated with the SOA. This is possible by the relevant fabrication process, where instead of a bulk implementation, the ODI is built using passive optical waveguide technology.<sup>17</sup> This technology minimizes the coupling and propagation losses to an extent that the overall IL can be kept below 3 dB.<sup>18</sup> Finally, where necessary, polarization controllers (PC), optical bandpass filters (OBPF), and isolators (ISO) can be used to properly align

the modulated light's polarization state, cut off the out-of-band noise, and ensure unidirectional propagation without back reflections, respectively.

## 3 Results

The average power of the pulses injected into the SOA was -2 dBm, which brought it into deep saturation. The difference between the pulse repetition period and the full-width at half-maximum pulsewidth was less than the SOA gain recovery time. These operating conditions are capable of provoking a pronounced pattern effect at the SOA output. When the amplified signal is introduced in the ODI from port 1 of the first coupler, it splits into two beams of equal intensity that travel along its two arms. Due to their relative delay, the beams reach the other end of the ODI at different times, which creates a phase difference between them given by  $\Delta\phi = (2\pi c\Delta\tau)/\lambda$ , where  $c$  is the speed of light in vacuum, and  $\lambda = 1550$  nm.<sup>14</sup> Thus, when they recombine at port 2 varies periodically with  $\Delta\phi$  and subsequently  $\lambda$ . This is shown in Fig. 2(a), which was obtained by connecting a broadband white light source to the ODI input and measuring the output with an optical spectrum analyzer (OSA) of 0.06-nm resolution bandwidth.

The transfer function of the ODI consists of alternating maxima and minima depending on whether  $\Delta\phi$  is an even or an odd multiple of  $\pi$ , respectively. The wavelength spacing between adjacent peaks or the free spectral range (FSR) is approximately 5.4 nm, which allows us to calculate from  $\text{FSR} = (\lambda^2)/(c\Delta\tau)$  the value of the employed time delay,  $\Delta\tau = 1.48$  ps.<sup>14</sup> Because of this form, the ODI can act as a notch filter and suppress the spectral components of the amplified pulses that have been spread toward the longer sideband.<sup>15</sup> This is shown in Fig. 2(c), in contrast with that in Fig. 2(b) before the SOA. This result can be achieved by biasing, with the appropriate choice of  $\Delta\tau$ , the ODI at the quadrature point with negative slope versus the optical carrier wavelength in the transmission characteristic.<sup>19</sup> In this manner, these spectral components are forced to lie close to the null points, which are located at the middle of the FSR and have a maximum relative attenuation of 14 dB. Consequently, the ODI eliminates the most red-shifted part of the spectrum, as shown in Fig. 2(d), which is associated with the pattern-dependent distortion caused by strong gain saturation.<sup>15</sup>

In the time domain, the signal emerging from the SOA is arranged by means of  $\Delta\tau$  to interfere with its delayed replica at output port 2 of the ODI. The interference is destructive when the incoming pulses encounter a partially recovered gain and constructive when they experience a more saturated gain.<sup>11</sup> This process causes the higher amplitudes to be clamped and the lower ones to be comparatively enhanced so that the variations in their peaks are balanced. The experimental results, obtained using a digital communications analyzer (DCA) with a 65-GHz optical bandwidth, are shown in the left column of Fig. 3. For a representative 20-bit-long sequence 11000110100101110111. [Fig. 3(a)] contained in the 10 Gb/s RZ 2<sup>7</sup>-1 PRBS, the intense amplitude excursions governing this stream after the SOA [Fig. 3(b)] are considerably smoothed by the ODI [Fig. 3(c)]. This improvement is quantified in terms of the

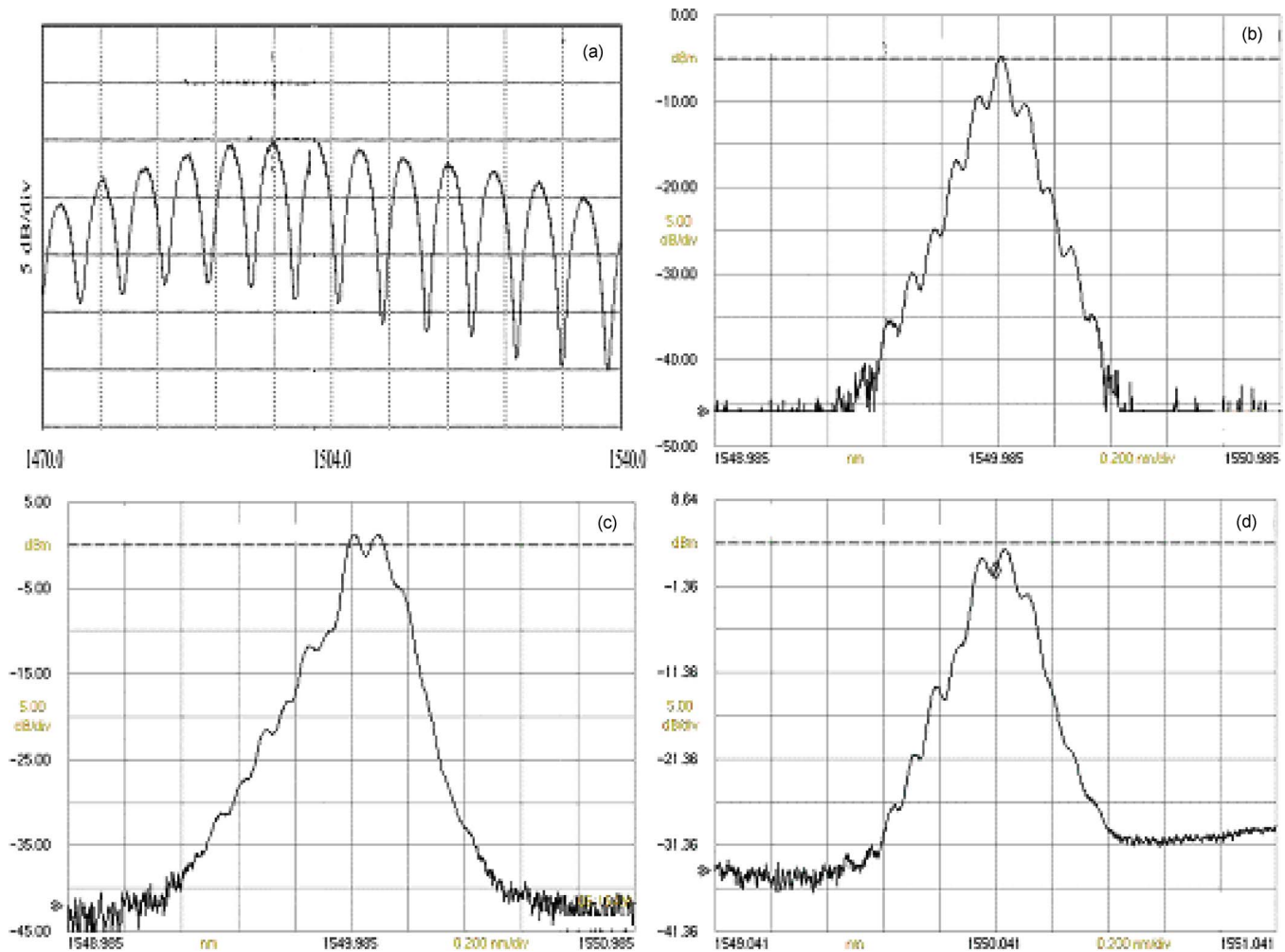


Fig. 2 Measured optical spectra: (a) ODI response, (b) SOA input, (c) SOA output, (d) after ODI.

amplitude modulation (AM), which is defined as the ratio between the maximum ( $P_{\max}^1$ ) and the minimum ( $P_{\min}^1$ ) peak power of the 1's in the considered PRBS sample, i.e.,  $AM = 10 \log(P_{\max}^1/P_{\min}^1)$ .<sup>11</sup> In order for the 1's to be uniform to a sufficient degree, the value of this metric must be below 1 dB.<sup>11</sup> In fact, with the use of the ODI, the AM decreased from 1.6 to 0.29 dB. According to the SOA specification data and the power level of its driving signal, this is achieved for an input power dynamic range extension of 5 dB. This improvement is also reflected on the quality of the eye diagrams illustrated in the right column of Fig. 3. Figure 3(b) shows severe degradation after the SOA with a poor extinction ratio (ER) of 10.5 dB. Figure 3(c) shows restoration by the ODI with an ER of 13.1 dB and resembles Fig. 3(a) before the SOA with the ER=15.6 dB. This figure of merit is defined<sup>20</sup> as the ratio between the maximum peak power of the 1's ( $P_{\max}^1$ ) to the maximum peak power of the 0's ( $P_{\max}^0$ ) measured by the DCA across the PRBS, i.e.,  $ER = 10 \log(P_{\max}^1/P_{\max}^0)$ . For an acceptable performance, this figure must be well above 10 dB. It is noteworthy that not only was the AM of the amplified pulses reduced, but that of the original pulses as well, from 0.42 to 0.29 dB. Thus, the combination of an SOA fol-

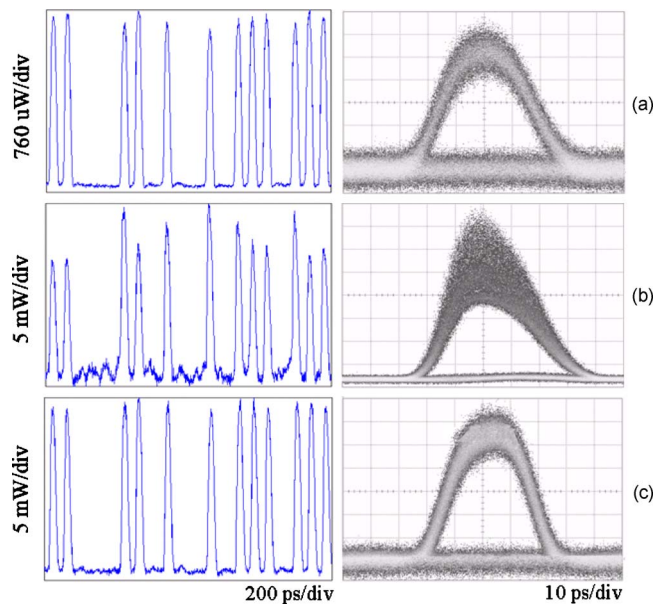


Fig. 3 Temporal waveforms at (a) SOA input, (b) SOA output, and (c) after ODI. Left column: PRBS sample of 20 bits, right column: eye diagrams.

lowed by an ODI can effectively reamplify and reshape the information-carrying signal and therefore has a regeneration effect. This is particularly important when cascading several SOAs,<sup>21</sup> because it impedes the peak amplitude differences between the amplified pulses to be accumulated from stage to stage that otherwise would be detrimental to the performance of an optical transmission system.

The achievement of the required interference at the output coupler was not an easy task. The differential phase shift imparted from the uneven lengths of the ODI branches drifted during the experiment due to changes in the environmental conditions. Thus, the scheme had error-free operation only within a very short time slot. However, this issue was not a matter of the concept but of its implementation. The ODI can be held at quadrature, by using a thermoelectric cooler to control the phase difference through fine-tuning of the operating temperature for a fixed signal wavelength,<sup>9</sup> or by using a feedback circuit to keep track of the path delay changes and make necessary microadjustments.<sup>19</sup> The stability of the scheme can be further enhanced if the ODI is fabricated using Si-SiO<sub>2</sub> waveguide technology<sup>14</sup> or is monolithically integrated with the SOA in a fully packaged module.<sup>16</sup>

#### 4 Conclusion

The capability of an ODI to reduce the pattern-dependent distortion induced on RZ data when amplified by an SOA has been experimentally demonstrated. The achievement of significant performance improvements compared to the SOA alone suggests that the proposed scheme constitutes an efficient solution for compensating the pattern effect on this pulse format.

#### References

1. Y. Kim, H. Jang, Y. Kim, J. Lee, D. Jang, and J. Jeong, "Transmission performance of 10-Gb/s 1550-nm transmitters using semiconductor optical amplifiers as booster amplifiers," *J. Lightwave Technol.* **21**(2), 476–481 (2003).
2. R. G.-Castrejón and A. Filios, "Pattern-effect reduction using a cross-gain modulated holding beam in semiconductor optical in-line amplifier," *J. Lightwave Technol.* **24**(12), 4912–4917 (2006).
3. M. Kumar, A. K. Sharma, and T. S. Kamal, "10 Gbps optical soliton transmission link using in-line SOA on standard SMF at 1.3  $\mu\text{m}$ ," *Optik* **118**(1), 34–37 (2007).
4. S. Singh and R. S. Kaler, "Power budget improvement for long-haul WDM transmission with optimum placement of SOAs," *Optik* **119**(7), 329–339 (2008).
5. R. Gutiérrez-Castrejón, L. Schares, and M. Duell, "SOA nonlinearities in 4  $\times$  25 Gb/s WDM pre-amplified system for 100-Gb/s Ethernet," *Opt. Quantum Electron.* **40**(13), 1005–1019 (2008).
6. M. J. Connelly, *Semiconductor Optical Amplifiers*, Kluwer Academic Press, Boston (2002).
7. Q. Xu, M. Yao, Y. Dong, W. Cai, and J. Zhang, "Experimental demonstration of pattern effect compensation using an asymmetrical Mach-Zehnder interferometer with SOAs," *IEEE Photon. Technol. Lett.* **13**(12), 1325–1327 (2001).
8. K. Chan, C.-K. Chan, W. Hung, F. Tong, and L. K. Chen, "Waveform restoration in semiconductor optical amplifier using fiber loop mirror," *IEEE Photon. Technol. Lett.* **14**(7), 995–997 (2002).
9. C. S. Wong and H. K. Tsang, "Reduction of bit-pattern dependent errors from a semiconductor optical amplifier using an optical delay interferometer," *Opt. Commun.* **232**(1–6), 245–249 (2004).
10. M. Kumar, A. K. Sharma, T. S. Kamal, and J. S. Malhotra, "Comparative investigation and suitability of various data formats for 10 Gb/s optical soliton transmission links at different chirps," *Optik* **120**(7), 330–336 (2009).
11. K. E. Zoiros, T. Siarkos, and C. S. Koukourlis, "Theoretical analysis of pattern effect suppression in semiconductor optical amplifier utilizing optical delay interferometer," *Opt. Commun.* **281**(14), 3648–3657 (2008).
12. K. E. Zoiros, C. O'Riordan, and M. J. Connelly, "Semiconductor optical amplifier pattern effect suppression using Lyot filter," *Electron. Lett.* **45**(23), 1187–1188 (2009).
13. K. E. Zoiros, C. O'Riordan, and M. J. Connelly, "Semiconductor optical amplifier pattern effect suppression using a birefringent fiber loop," *IEEE Photon. Technol. Lett.* **22**(4), 221–223 (2010).
14. H. Dong, G. Zhu, Q. Wang, H. Sun, N. K. Dutta, J. Jaques, and A. B. Piccirilli, "Multiwavelength fiber ring laser source based on a delayed interferometer," *IEEE Photon. Technol. Lett.* **17**(2), 303–305 (2005).
15. K. Inoue, "Optical filtering technique to suppress waveform distortion induced in a gain-saturated semiconductor optical amplifier," *Electron. Lett.* **33**(10), 885–886 (1997).
16. J. Leuthold, C. H. Joyner, B. Mikkelsen, G. Raybon, J. L. Pleumeekers, B. I. Miller, K. Dreyer, and C. A. Burrus, "100 Gbit/s all-optical wavelength conversion with integrated SOA delayed-interference configuration," *Electron. Lett.* **36**(13), 1129–1130 (2000).
17. A. Bhardwaj, N. Sauer, L. Buhl, W. Yang, L. Zhang, and D. T. Neilson, "An InP-based optical equalizer monolithically integrated with a semiconductor optical amplifier," *IEEE Photon. Technol. Lett.* **19**(19), 1514–1516 (2007).
18. J. Leuthold, C. H. Joyner, B. Mikkelsen, G. Raybon, J. L. Pleumeekers, B. I. Miller, K. Dreyer, and C. A. Burrus, "Compact and fully packaged wavelength converter with integrated delay loop for 40 Gbit/s RZ signals," *Proc. Optical Fiber Communication Conference (PD17)*, 1–4 (2000).
19. D. Derickson, *Fiber Optic Test and Measurement*, Prentice Hall Professional Technical Reference, New Jersey (1997).
20. K. Hinton, G. Raskutti, P. M. Farrell, and R. S. Tucker, "Switching energy and device size limits on digital photonic signal processing technologies," *IEEE J. Sel. Top. Quantum Electron.* **14**(3), 938–945 (2008).
21. S. Singh and R. S. Kaler, "Transmission performance of 20  $\times$  10 Gb/s WDM signals using cascaded optimized SOAs with OOK and DPSK modulation formats," *Opt. Commun.* **266**(1), 100–110 (2006).

Biographies and photographs of authors not available.